Archives of Microbiology (2024) 206:404
https://doi.org/10.1007/s00203-024-04136-8

ORIGINAL PAPER

Baicalein induces apoptosis by targeting ribosomes in *Candida auris*

Can Li[1,2] · Jun Wang[3] · Hui Wu[1,2] · Long Zang[1,2] · Wei Qiu[1,2] · Wenfan Wei[1,2] · Tianming Wang[1,2] · Changzhong Wang[1,2]

Received: 15 July 2024 / Revised: 28 August 2024 / Accepted: 8 September 2024

Abstract

The emergence of the "super fungus" *Candida auris* poses a significant threat to human health, given its multidrug resistance and high mortality rates. Therefore, developing a new antifungal strategy is necessary. Our previous research showed that Baicalein (BE), a key bioactive compound from the dried root of the perennial herb *Scutellaria baicalensis* Georgi, has strong fungistatic properties against *C. auris*. Nevertheless, the antifungal activity of BE against *C. auris* and its mechanism of action requires further investigation. In this study, we explored how BE affects this fungus using various techniques, including scanning electron microscopy (SEM), Annexin V-FITC apoptosis detection, CaspACE FITC-VAD-FMK In Situ Marker, reactive oxygen species (ROS) assay, singlet oxygen sensor green (SOSG) fluorescent probe, enhanced mitochondrial membrane potential (MMP) assay with JC-1, DAPI staining, TUNEL assay and reverse transcription–quantitative polymerase chain reaction (RT-qPCR). Our findings revealed that BE induced several apoptotic features, including phosphatidylserine (PS) externalization, metacaspase activation, nuclear condensation and DNA fragmentation. BE also increased intracellular ROS levels and altered mitochondrial functions. Additionally, transcriptomic analysis and RT-qPCR validation indicated that BE may induce apoptosis in *C. auris* by affecting ribosome-related pathways, suggesting that ribosomes could be new targets for antifungal agents, in addition to cell walls, membranes, and DNA. This study emphasizes the antifungal activity and mechanism of BE against *C. auris*, offering a promising treatment strategy for *C. auris* infection.

Can Li and Jun Wang are co-first authors.

Communicated by Yusuf Akhter.

✉ Changzhong Wang
ahwcz63@sina.com

[1] Department of Pathogenic Biology and Immunology, College of Integrated Chinese and Western Medicine, (College of Life Science), Anhui University of Chinese Medicine, No. 350 Longzihu Road, Xinzhan District, Hefei 230012, China

[2] Institute of Integrated Traditional Chinese and Western Medicine, Anhui University of Chinese Medicine, Hefei, China

[3] Anhui Provincial Institutes for Food and Drug Control, Hefei, China

Published online: 16 September 2024

Graphical Abstract

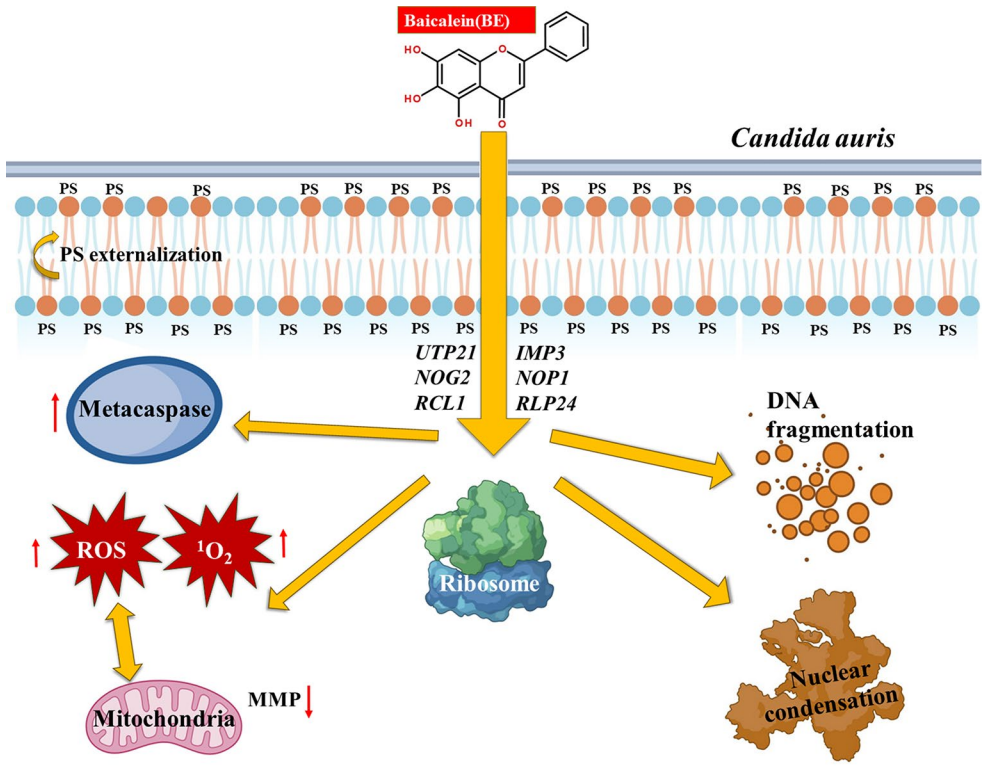

Schematic representation of this study. Baicalein (BE) triggers apoptosis in *Candida auris* by affecting ribosome-related pathways. This action leads to several apoptotic characteristics, such as phosphatidylserine (PS) externalization, metacaspase activation, nuclear condensation, DNA fragmentation, increased levels of ROS and $^1O_2$, and alterations in mitochondrial membrane potential (MMP)

Keywords *Candida auris* · Baicalein · Apoptosis · Transcriptomics · Ribosome

Abbreviations

AmB	Amphotericin B
BE	Baicalein
C. auris	Candida auris
C. albicans	Candida albicans
DCFH-DA	2',7'-Dichlorodihydrofluorescein diacetate
DDR	DNA damage response
DR4	Death receptor 4
FLZ	Fluconazole
GO	Gene Ontology
KEGG	Kyo-to Encyclopedia of Genes and Genomes
MDS	Myelodysplastic syndrome
MMP	Mitochondrial membrane potential
mROS	Mitochondrial reactive oxygen species
PBS	Phosphate buffered saline
PCD	Programmed cell death
PS	Phosphatidylserine
ROS	Reactive oxygen species
RP	Ribosomal protein
rRNA	Ribosomal RNA
RSR	Ribotoxic stress response
Rt-qPCR	Reverse transcription–quantitative polymerase chain reaction
snoRNP	Small nucleolar ribonucleoprotein
SEM	Scanning electron microscope
SOSG	Singlet oxygen sensor green
TRAIL	Tumor necrosis factor-related apoptosis-inducing ligand
WHO FPPL	WHO fungal priority pathogens list
YPD	Yeast Peptone Dextrose

Introduction

Candida auris, first identified in Japan in 2009, has emerged as a significant threat to public health (Satoh et al. 2009). *C. auris* is a yeast that causes invasive candidiasis, a

life-threatening disease with high mortality rates. *C. auris* can cause outbreaks and has already led to several hospital outbreaks worldwide (Ahmad et al. 2020). It is resistant to most antifungal medications, including azoles, polyenes, and echinocandins, with some strains being pan-resistant. *C. auris* is classified as a critical priority pathogen on the WHO's fungal priority pathogens list (WHO FPPL) (Bing et al. 2024).

Currently, the strong drug resistance of *C. auris* limits the available treatment options for its infection. Our previous studies have demonstrated that baicalein (BE) has the potential to be a new antifungal and anti-biofilm agent. Results indicate that BE effectively inhibits the growth, adhesion, and biofilm formation of *C. auris*. It also reduced drug resistance and aggregation by disrupting the cell membrane and cell wall, as well as decreasing colonization and invasion of the host. We showed that BE effectively inhibits multidrug-resistant *C. auris* through in vitro phenotypic and genotypic analyses, along with preliminary signs of BE-induced apoptosis. However, further research is needed to understand how BE works against *C. auris* at a mechanistic level. (Li et al. 2024). Apoptosis, a form of programmed cell death, is present in both multicellular and unicellular organisms. (Kaczanowski. 2016). Apoptosis is characterized by several hallmarks, including PS externalization, DNA fragmentation, nuclear condensation, metacaspase activation, ROS and $^1O_2$ accumulation, and loss of mitochondrial membrane potential (MMP) (Jia et al. 2019). Previous research has demonstrated that baicalein (BE) is capable of inducing apoptosis in *Candida albicans*. Upon exposure to 14.8 µM BE for 12 h, the cells of *C. albicans* underwent apoptosis. Furthermore, an increase in intracellular levels of ROS and the upregulation of redox-related genes (*CAP1*, *SOD2*, *TRR1*) were observed. Additionally, there was a significant change in the MMP of *C. albicans* cells upon BE treatment. These findings indicate that BE treatment induces apoptosis in *C. albicans* cells by disrupting the MMP (Dai et al. 2009). Further research has also demonstrated that the combination of BE and Amphotericin B (AmB) accelerates *C. albicans* apoptosis, concomitant with an increase in ROS (Fu et al. 2011). Therefore, we were intrigued by the potential of BE to induce apoptosis in *C. auris*.

To elucidate the mechanism of BE-induced apoptosis in *C. auris*, we conducted transcriptomic analysis. The results indicated a significant link between ribosome activity and apoptosis in *C. auris* under these conditions. Ribosomes are cellular organelles responsible for mediating protein translation, which is one of the most energy-demanding activities within the cell. Eukaryotic ribosomes are made up of two subunits: 40 S and 60 S, which include ribosomal proteins and ribosomal RNA (rRNA). In addition to translation, ribosomal proteins also play roles in various extra ribosomal functions, such as cell apoptosis (Liu et al. 2024). Malfunctions in ribosomes can trigger ribotoxic stress response (RSR), impairing protein synthesis and reducing cell viability (Sinha et al. 2024). A study demonstrated that both MMP and mitochondrial reactive oxygen species (mROS) levels increased in response to ribosomal impairments (Liu et al. 2024); Ribosomal protein (RP) L23 negatively regulates cellular apoptosis. In patients with higher-risk myelodysplastic syndrome (MDS), CD34+ cells exhibit abnormal resistance to apoptosis due to the overexpression of RPL23. It has been observed that reduced RPL23 expression led to suppressed cellular viability, increased apoptosis, and G1-S cell cycle arrest (Qi et al. 2017); Unphosphorylated RPS6 induces apoptosis by increasing the expression of death receptor 4 (DR4), which is part of the mechanism of tumor necrosis factor-related apoptosis-inducing ligand (TRAIL) (Yi et al. 2021).

In conclusion, ribosomes are closely linked to apoptosis. This study explored how BE combats *C. auris* by examining various apoptotic markers after treatment, using the ribosomal gene set pathway identified through transcriptome sequencing.

Materials and methods

Candida auris strain and cultivation

The *C. auris* strain was obtained from Prof. Huang Guanghua at FuDan University. After culturing on Yeast Peptone Dextrose (YPD) Agar, the C. auris was activated in YPD Broth and then incubated at 37 °C for 12 h until reaching the exponential phase. The fungal precipitate was collected by centrifugation at 825 × g for 5 min, and the supernatant was removed. RPMI-1640 medium (pH 7.0) was added to adjust the concentration to 2×10^6 CFU/ml. The *C. auris* suspensions were then treated with different concentrations of BE and FLZ, while a control group without medication was also included for comparison purposes. The methods outlined below all adhere to the experimental setup and conditions described. The following methods adhere to the experimental setup and conditions described above.

SEM

After cultured, non-adherent cells were rinsed with sterile phosphate buffered saline (PBS) buffer and then immersed in pre-chilled 2.5% glutaraldehyde for at least 2 h. The samples were then dehydrated in a series of ethanol concentrations (30%, 50%, 70%, 95%, and 100%) for 20 min. Following adequate air drying, the specimens were gold-coated, examined, and imaged using a Thermo Quattro S

scanning electron microscope. (Thermo Quattro S, Thermo Fisher Scientific, USA) (Li et al. 2024).

Analysis of phosphatidylserine (PS) externalization

Following the incubation process, the cells were then centrifuged at 1000 × g for 3–5 min and resuspended in fresh PBS, followed by two washes with PBS. Subsequently, the Annexin V-FITC apoptosis detection kit (Beyotime Biotechnology Co., Ltd., Shanghai, China) was used according to the manufacturer's instructions to determine the induction of apoptosis in cells using flow cytometry (BD FACSCelesta, USA) (Jia et al. 2019; Liu et al. 2022).

Metacaspase activation assay

After incubation, the fungal cells were collected and washed with sterile PBS. Subsequently, they were stained with 10μM CaspACE™ FITC-VAD-FMK In Situ Marker (Promega Biotech Co., Ltd., USA) at 37˚C for 25–30 min in the dark. Fluorescence was examined using a DMi8 microscope (Leica, Wetzlar, Hesse, Germany) at ×630 magnification (Liu et al. 2022).

ROS

Following the incubation period, Samples were stained using the ROS Assay Kit (Beyotime Biotechnology Co., Ltd, Shanghai, China) for 20 min at 37 °C. Excess 2',7'-Dichlorodihydrofluorescein diacetate (DCFH-DA) was removed with sterile PBS (Liu et al. 2022; Lei et al. 2023). Fluorescence was observed using a DMi8 microscope at ×630 magnification.

SOSG

After incubation, non-adherent fungal cells were removed by rinsing with sterile PBS. Subsequently, Singlet oxygen sensor green (SOSG, Maokang Biotechnology Co., Ltd, Shanghai, China) was added at concentration of 10 μM, and the cells were stained for 30 min under light protection (Liu et al. 2022). Fluorescent expression was observed using a DMi8 microscope at ×630 magnification.

Mitochondrial membrane potential assay

After being cultured, the cells were subsequently centrifuged at 1000 × g for 3–5 min and then resuspended in fresh PBS, followed by three washes with PBS. Following this, the enhanced mitochondrial membrane potential assay kit with JC-1(Beyotime Biotechnology Co., Ltd, Shanghai, China) was utilized as per the manufacturer's instructions to measure the MMP. After being washed in PBS, the cells were analyzed using flow cytometry. The ratio of fluorescence intensities of aggregates JC-1 to monomer was calculated (Jia et al. 2019).

Detection of nuclear condensation

After incubation, the treated cells were washed with PBS two times and stained with DAPI (Sparkjade Biotechnology Co., Ltd., Shandong, China) at a concentration of 10 μg/ml for 10 min in the dark (Tian et al. 2017; Jia et al. 2019; Liu et al. 2022). Subsequently, the samples were examined using a DMi8 microscope at a magnification of ×630.

Determination of DNA fragmentation

Following the incubation period, the cells were washed with PBS two times and stained with a One Step TUNEL Apoptosis Assay Kit (Beyotime Biotechnology Co., Ltd., Shanghai, China) for 60 min at 37˚C (Tian et al. 2017; Jia et al. 2019; Liu et al. 2022). Finally, the apoptotic cells were assessed by DMi8 microscope at a magnification of ×630.

Transcriptome sequencing

Firstly, total RNA was extracted from *C. auris* in the control group (n = 3) and the BE (59.2 μM) group (n = 3), and the concentration and purity of the RNA were assessed using Nanodrop2000. The integrity of the RNA was evaluated through agarose gel electrophoresis, and the RQN value was determined with Agilent5300. Subsequently, mRNA was isolated from total RNA by A-T base pairing of ploy A with magnetic beads containing Oligo (dT). Following fragmentation in suitable conditions, the mRNA fragments were reverse transcribed into one-strand cDNA using random primers and reverse transcriptase. This single-stranded cDNA then underwent two-strand synthesis to form a stable double-stranded structure. The double-stranded cDNA ends were repaired to create blunt ends using End Repair Mix, followed by addition of an A base at the 3' end to facilitate adapter ligation. After purification and separation of adapter-ligated products, PCR amplification was performed to generate final library for sequencing on a computer (Wu et al. 2024). In GO analysis, the software Goatools was employed for enrichment analysis, and the Fisher exact test was utilized. To control the calculated false positive rate, four multiple test approaches (Bonferroni, Holm, Sidak, and false discovery rate) were adopted to correct the P-value. Generally, when the corrected P-value (p_fdr) < 0.05, it is regarded that there is significant enrichment of GO function. The Python scipy software package was employed for KEGG PATHWAY enrichment analysis. The calculation

principle was consistent with that of GO functional enrichment analysis, and the Fisher exact test was utilized for the calculation. To control the calculation of the false discovery rate, the BH(FDR) method was adopted for multiple tests, and a Corrected P-Value of 0.05 was set as the threshold. KEGG pathways fulfilling this condition were defined as those that were significantly enriched in differentially-expressed genes. The software for cluster analysis is fastcluster.

RT-qPCR

The cDNA extracted from *C. auris* was utilized for cDNA synthesis according to the manufacturer's instructions for the reverse transcription kit (Yeasen Biotechnology Co., Ltd., Shanghai, China). The primer sequences are presented in Table 1. RT-qPCR amplification was performed using a Light Cycler ® 96 for fluorescence quantification, with an initial denaturation at 95 °C for 5 min, followed by 40 cycles of denaturation at 95 °C for 10 s, annealing at 50–60 °C for 20 s, and extension at 72 °C for 20 s. Gene expression levels were assessed using the relative quantification method based on cycle threshold values (2-ΔΔCt). (Wu et al. 2023).

Statistical analysis

The data presented represent the average value ± the standard deviation from a minimum of three biological replicates. Statistical analysis was performed using Graphpad Prism 9.5 and SPSS 23.0, with the application of one-way ANOVA followed by LSD or Welch's method. Statistical significance was considered at $P < 0.05$.

Table 1 Primers sequences used for RT-qPCRPrimers sequences used for RT-qPCR

Gene	Primer sequences
C. auris-ACT1	Forward (5'-3'): GTCGGTGATGAGGCTCAATCCAAG
	Reverse (5'-3'): GTCGTCCCAGTTCGTGACAATACC
C. auris-IMP3	Forward (5'-3'): GGTGTGGTGATGTGTCGTCTTCG
	Reverse (5'-3'): ACCCACGTTAGGTAGTCCTCCAAG
C. auris-NOP1	Forward (5'-3'): TGGTGGTGCTCGTGGTGGTC
	Reverse (5'-3'): AGCGTGTCTGTGAGGTTCAATGAC
C. auris-UTP21	Forward (5'-3'): TCGGACACAGCAACAGAATCACAG
	Reverse (5'-3'): CACGTTAGGAAGGCGGATACCATC
C. auris-NOG2	Forward (5'-3'): GCCAGATGAGAGTGCGGTTGC
	Reverse (5'-3'): TCTTCGCCTGTTCTCACCTCCTC
C. auris-RCL1	Forward (5'-3'): AACAAGCTCCGACAGCACAAGAG
	Reverse (5'-3'): GACTTCACCACCGCCCAAAGG
C. auris-RLP24	Forward (5'-3'): GCTGCTAGAAGAAACGTCCCTGTC
	Reverse (5'-3'): GCCTCTCCTTGTTGCCTCTCATTC

Results

BE inhibits the formation of C. Auris biofilm

C. auris exhibited a distinct oval-shaped yeast morphology in both the control group and the groups treated with 7.4 μM and 14.8 μM BE, as well as 209 μM FLZ. Moreover, exposure to BE at concentrations of 29.6 μM and 59.2 μM caused noticeable changes in yeast cell shape, suggesting a reduced ability to divide. Additionally, we observed a decrease in the number of *C. auris* as BE concentration increased (Fig. 1).

BE triggers PS externalization results in viable apoptosis

PS is typically located on the inner side of the plasma membrane, but in apoptotic and necrotic cells, PS becomes exposed on the outer surface. Therefore, PS is considered an early marker of apoptosis in fungi. Annexin V has a specific affinity for externalized PS, while PI only stains damaged cells. Viable apoptotic cells are identified as Annexin V-FITC+/PI-, whereas non-viable apoptotic and necrotic cells are labeled as Annexin V-FITC+/PI+.

In our study, the control groups had a large population of viable cells, with only 3.98% showing staining for apoptotic cells, highlighting the contrast with the increased apoptosis observed after treatment. Following treatment with various concentrations of BE and FLZ, there was an increase in the number of cells in the Annexin V+/PI- and Annexin V-FITC+/PI + quadrants. *C. auris* cells treated with 29.6 μM and 59.2 μM BE showed significant apoptotic populations of 39.9% and 41.23%, respectively, indicating that BE induced apoptosis in *C. auris* (Fig. 2).

BE induces metacaspase activation

Metacaspases are caspase-like cysteine proteases found in yeast that play a crucial role in the early stages of apoptosis and can be detected using FITC-VAD-FMK staining. Cells with activated intracellular metacaspases exhibit green fluorescence, whereas control cells show no staining. The study showed that fluorescence intensity increased with higher concentrations of BE (14.8, 29.6, and 59.2 μM), indicating elevated metacaspase activity in BE-treated cells, but not in FLZ-treated cells (Fig. 3).

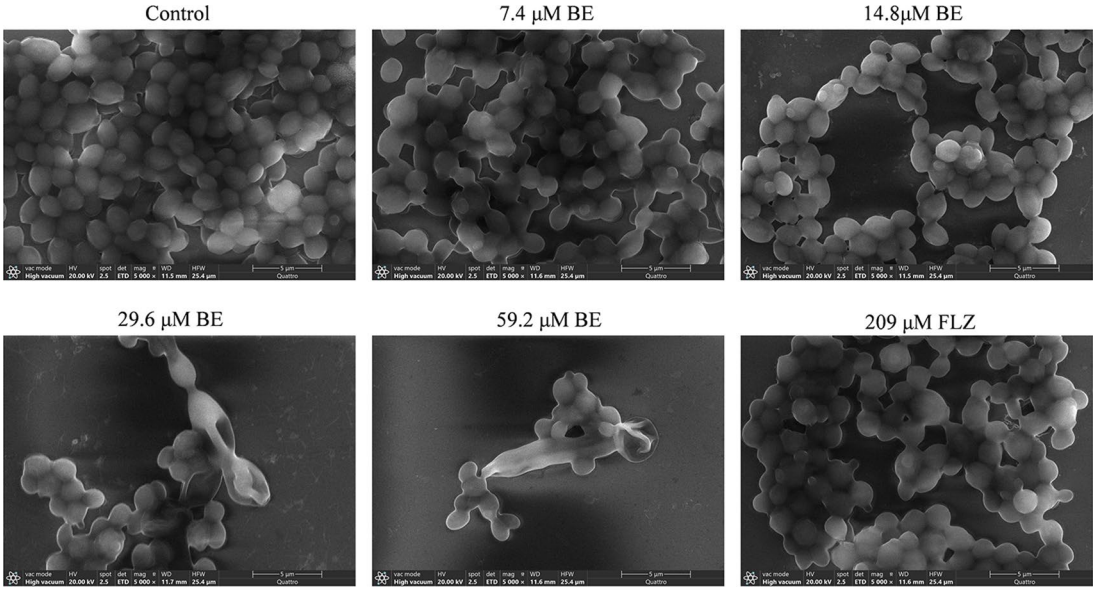

Fig. 1 Baicalein (BE) disrupts the morphological architecture of *C. auris* biofilm. Images depict the biofilms of *C. auris* under scanning electron microscope (SEM) examination

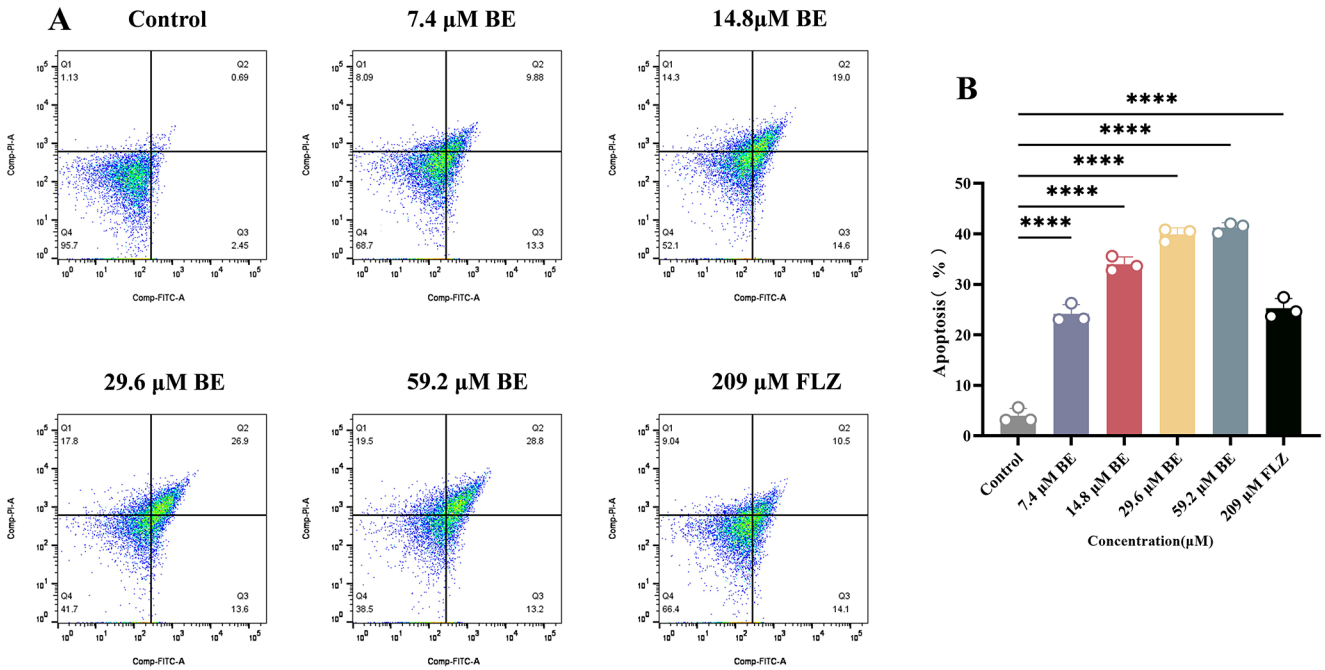

Fig. 2 Baicalein (BE) triggers the externalization of phosphatidylserine (PS), resulting in viable apoptosis. (**A**) Images represent results of flow cytometry. (**B**) Histogram displays quantification of the number of *C. auris* apoptosis by FlowJo. All data are presented as mean ± SD: ****$P < 0.0001$ vs. Control group

BE produces ROS accumulation

The production of ROS may directly damage yeast cells by inducing and regulating apoptosis. As depicted in Fig, the BE (29.6 and 59.2 μM) groups exhibited strong green fluorescence, while the other groups showed minimal fluorescence. This suggests that BE significantly increased fluorescence in a dose-dependent manner, indicating that BE caused ROS accumulation in *C. auris* (Fig. 4).

BE produces $^1O_2$ accumulation

The reactive oxygen species, $^1O_2$, could disrupt various biological cell components such as lipids, proteins, and nucleic

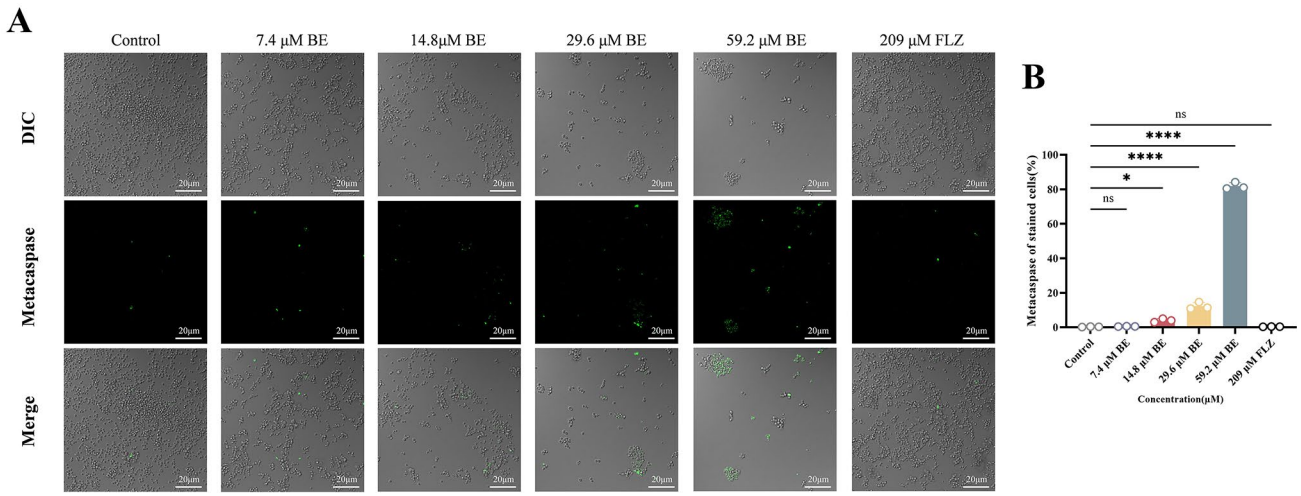

Fig. 3 Baicalein (BE) triggers metacaspase activation of *C. auris*. (**A**) Images represent the accumulation of metacaspase, with green fluorescence observed. Scale bars 20 μm. (**B**) Histogram displays the proportion of cells that are positive for metacaspase. Quantification of fluorescence-labeled *C. auris* number by Image J. All data are presented as mean ± SD: ns = not significant, $*P < 0.05$, $****P < 0.0001$ vs. Control group

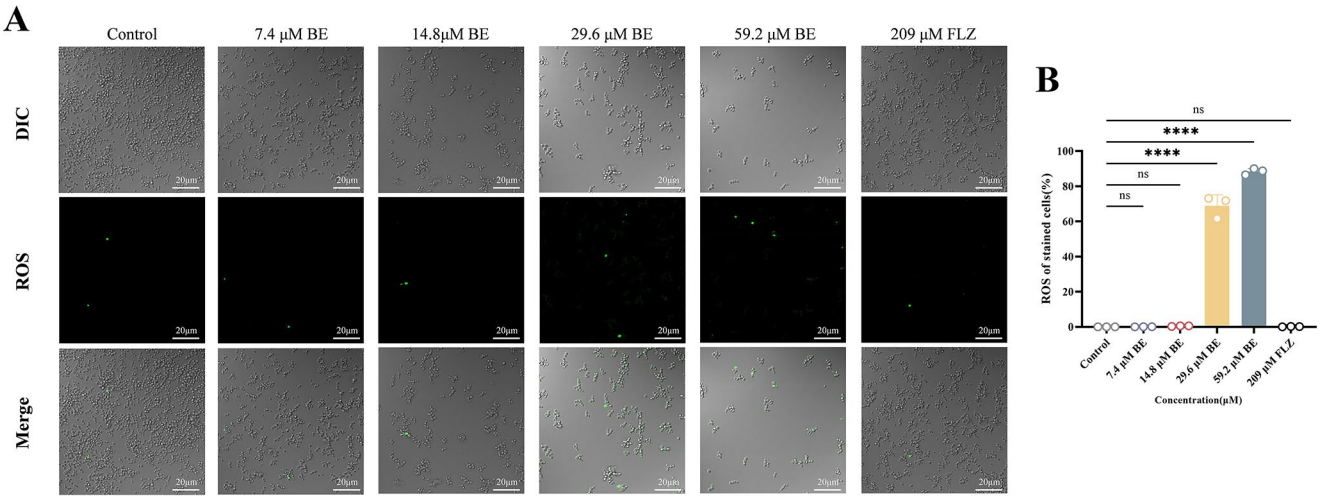

Fig. 4 Baicalein (BE) produces reactive oxygen species (ROS) accumulation. (**A**) Images represent the accumulation of ROS, with green fluorescence observed. (**B**) Histogram displays the proportion of cells that are positive for ROS. Quantification of fluorescence-labeled *C. auris* number by Image J. All data are presented as mean ± SD: ns = not significant, $****P < 0.0001$ vs. Control group

acids through cellular metabolism, REDOX reactions, and photoactivation. The production of intracellular $^1O_2$ was further assessed using SOSG stained *C. auris*, which emits a green fluorescence in the presence of singlet oxygen. As depicted in Fig, the BE (29.6 and 59.2 μM) group exhibited strong green fluorescence, while the other groups showed minimal fluorescence (Fig. 5). This result indicates that BE led to an accumulation of $^1O_2$ in *C. auris*.

BE disrupts mitochondrial membrane potential

Mitochondria are a crucial target of ROS. An abnormal rise in ROS levels usually causes mitochondrial damage and changes in the mitochondrial membrane potential. This alteration is considered the initial event of apoptosis. Typically, a high mitochondrial membrane potential (MMP) leads to the accumulation of JC-1 in the mitochondrial matrix, forming JC-1 aggregates that emit red fluorescence. In contrast, when MMP decreases, JC-1 exists as monomers, which produce green fluorescence. Our study revealed that in *C. auris* cells treated with BE, the ratio of JC-1 aggregates to monomers decreased in a concentration-dependent manner, indicating a loss of MMP and mitochondrial damage. Similar findings were also obtained for the FLZ group (Fig. 6).

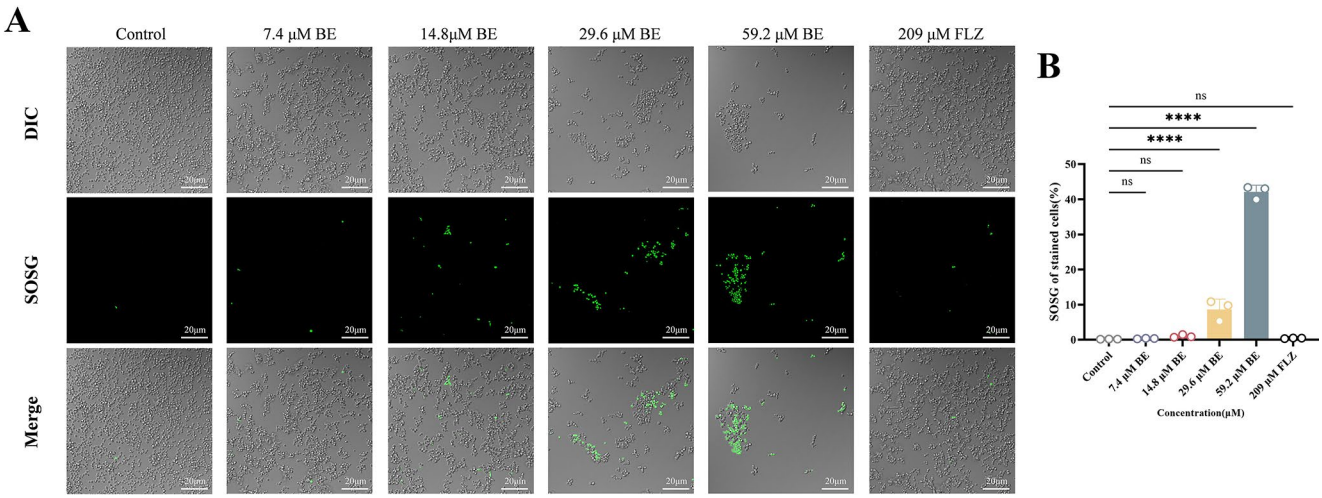

Fig. 5 Baicalein (BE) produces $^1O_2$ accumulation. (**A**) Images represent the accumulation of $^1O_2$, with green fluorescence observed. (**B**) Histogram displays the proportion of cells that are positive for $^1O_2$. Quantification of fluorescence-labeled *C. auris* number by Image J. All data are presented as mean ± SD: ns = not significant, ****$P < 0.0001$ vs. Control group

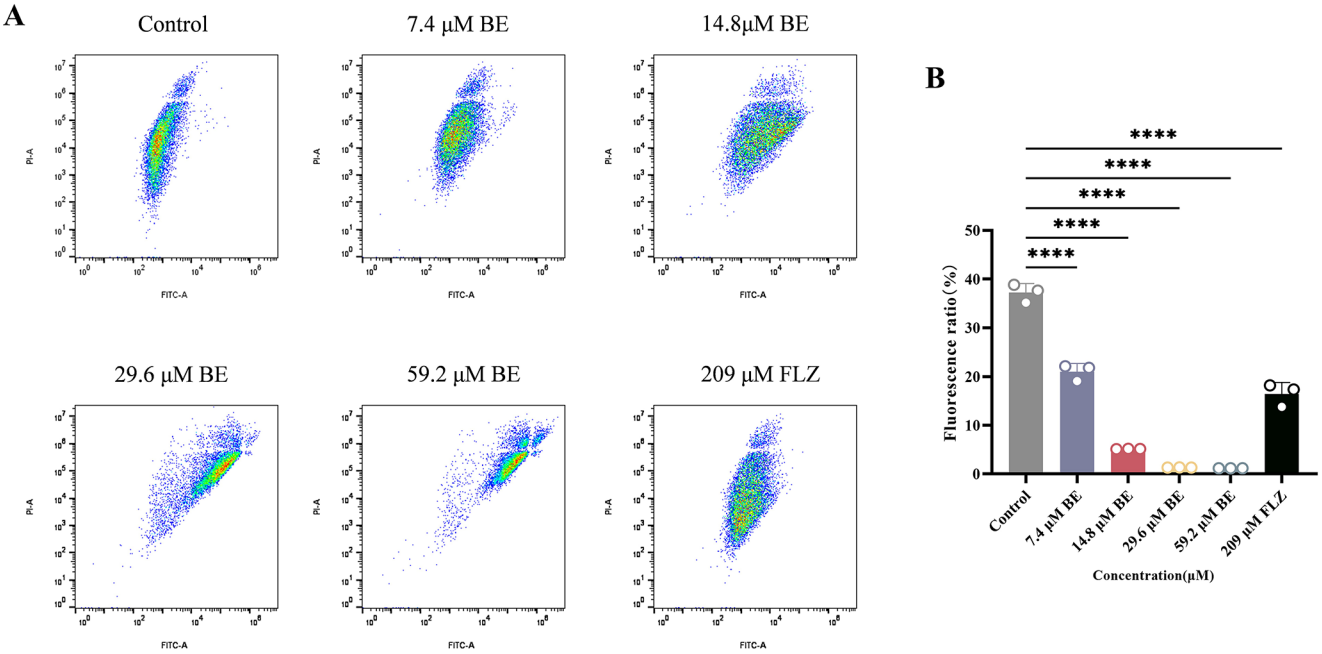

Fig. 6 Baicalein (BE) disrupts mitochondrial membrane potential (MMP). (**A**) Images represent results of flow cytometry. (**B**) Histogram displays quantification of MMP of *C. auris* by FlowJo. All data are presented as mean ± SD: ****$P < 0.0001$ vs. Control group

BE induces nuclear condensation

In comparison to the normal nucleus of the control and FLZ groups, the nucleus of BE (14.8,29.6 and 59.2 μM) treated yeasts exhibited a fragmented blue fluorescence or increased condensation, suggesting that BE induced nuclear condensation and fragmentation of *C. auris* (Fig. 7).

BE causes DNA fragmentation

Additionally, DNA fragmentation is recognized as a hallmark of apoptosis in the late phase. The TUNEL assay is commonly used to detect DNA fragmentation in cells, as it can identify apoptotic DNA cleavage by labeling fluorescent dUTP at the 3'-OH ends of DNA. Figure shows that there was a significant increase in fluorescence quantity in the BE (14.8,29.6 and 59.2 μM) groups, but not in the FLZ group, suggesting that BE caused DNA fragmentation (Fig. 8).

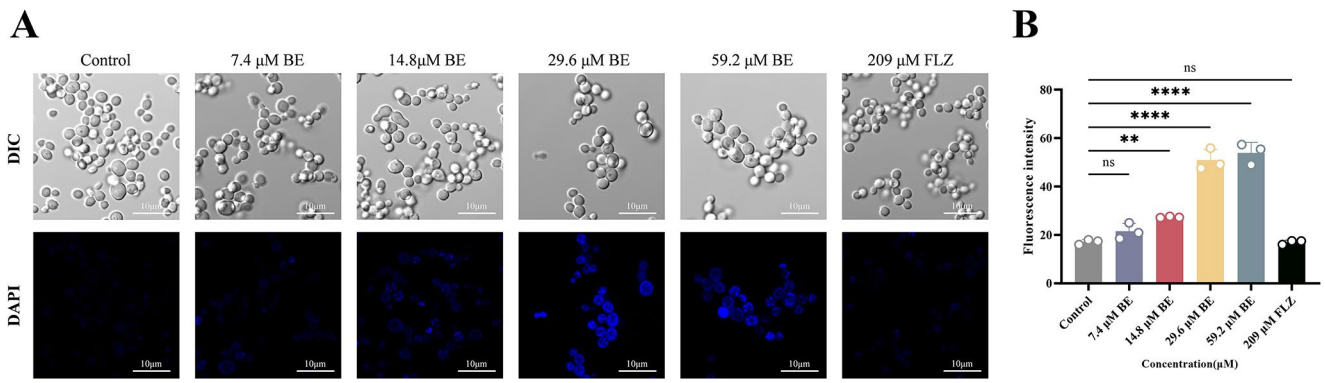

Fig. 7 Baicalein (BE) induces nuclear condensation. (**A**) Images represent the nuclear condensation of *C. auris*, with blue fluorescence observed. Scale bars 10 μm. (**B**) Histogram displays quantification of fluorescence intensity of *C. auris* stained with DAPI by Image J. All data are presented as mean ± SD: $^{**}P < 0.01$, $^{****}P < 0.0001$ vs. Control group

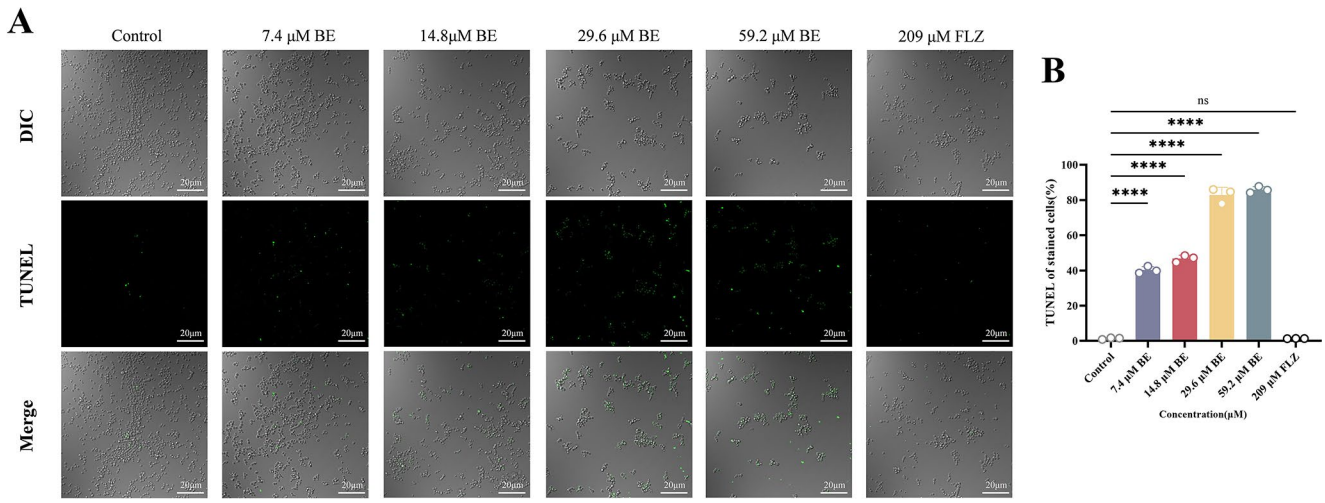

Fig. 8 Baicalein (BE) causes DNA fragmentation (**A**) Images represent the accumulation of DNA fragmentation, with green fluorescence observed. Scale bars 20 μm. (**B**) Histogram displays the proportion of cells that are positive for DNA fragmentation. Quantification of fluorescence-labeled *C. auris* number by Image J. All data are presented as mean ± SD: ns = not significant, $^{****}P < 0.0001$ vs. Control group

Transcriptomics and RT-qPCR results reveal BE regulated ribosome-related pathways

We sought to understand the molecular mechanisms of BE against *C. auris*. To achieve this, we performed transcriptome sequencing analysis on samples from the control and BE treatment groups using the Illumina high-throughput sequencing platform.

This research focused on genes with varying expression levels in the BE treatment group (59.2 μM) versus the control group. The analysis from the Kyoto Encyclopedia of Genes and Genomes (KEGG) indicated significant enrichment of differentially expressed genes in eukaryotic ribosome biogenesis and related processes. Among them, there are 54 differentially regulated genes in the ribosome biogenesis in eukaryotes pathway, and 58 differentially regulated genes in the ribosome pathway (Fig. 9A). The Gene Ontology (GO) enrichment analysis revealed the collective involvement of differentially expressed genes in the top 20 enriched pathways. Among these pathways, it was found that the induction of *C. auris* apoptosis by BE may be attributed to its influence on rRNA processing (112 differentially regulated genes), ncRNA processing (146 differentially regulated genes), rRNA metabolic process (114 differentially regulated genes), nucleolus (102 differentially regulated genes), preribosome (59 differentially regulated genes), ncRNA metabolic process(157 differentially regulated genes), cleavage involved in rRNA processing (30 differentially regulated genes), preribosome, and large subunit precursor (23 differentially regulated genes) (Fig. 9B). Clustering analysis of the associated genes, as depicted in the heatmap, indicated that BE had an impact on a range of ribosomal genes. (Fig. 9C-D).

To confirm the transcriptome results, we selected the six most differentially expressed genes (DEGs) from the two groups of ribosome-related genes for RT-qPCR. *IMP3* is a

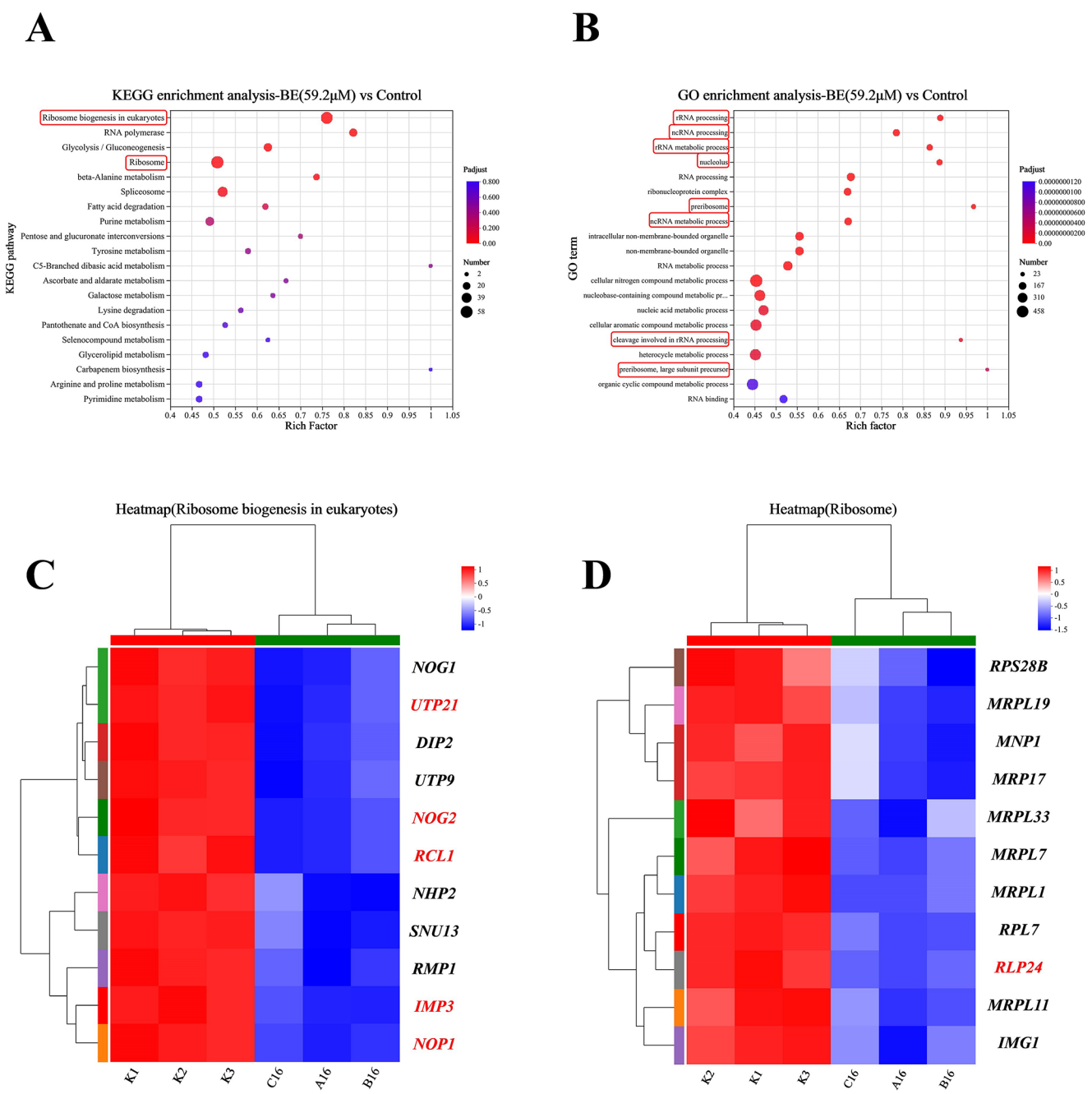

Fig. 9 Baicalein (BE) regulates the expression of ribosomal genes associated with *C. auris*. (**A**) Annotation analysis of KEGG function in the BE (59.2μM) group vs. control group. (**B**) GO functional enrichment analysis of the BE (59.2μM) group vs. control group. (**C**) Heatmap of clustering analysis of ribosome biogenesis in eukaryotes. (**D**) Heatmap of clustering analysis of ribosome

U3 small nucleolar ribonucleoprotein (snoRNP) that plays a crucial role in pre-rRNA processing. The snoRNP *NOP1* (fibrillarin) is essential for pre-rRNA processing in yeast and is vital for cell viability. *UTP21* is a protein component of UTPB, which is a large and evolutionarily conserved complex involved in the early processing of 18 S rRNA within the 90 S small subunit processome. Additionally, *NOG2* and *RLP24* are pre-ribosomal proteins that serve as critical regulators of ribosome biogenesis. *RCL1*, like the RNA 3'-phosphate cyclase in yeast, associates with U3 snoRNP and is required for 18 S rRNA biogenesis. The results demonstrated a significant downregulation of all genes under BE treatment, which is consistent with the transcriptome data (Fig. 10). This suggests that BE can have a significant impact on the ribosomal pathways of *C. auris*.

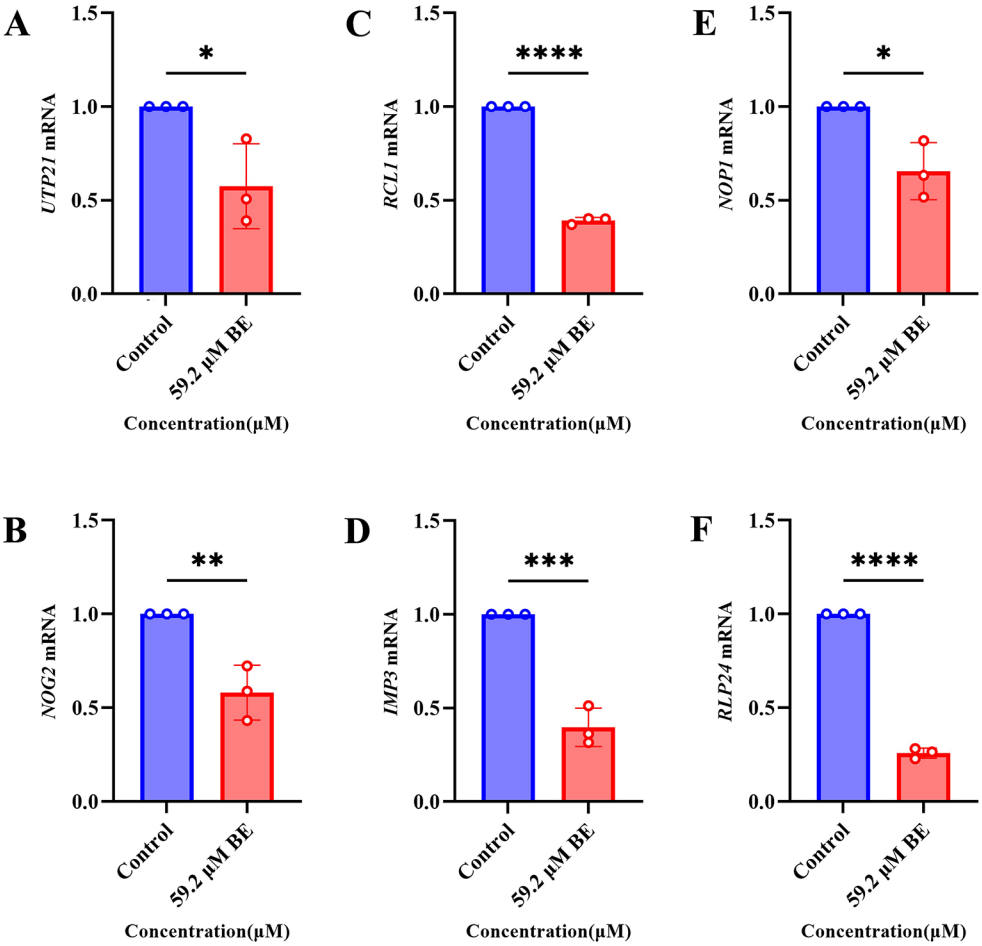

Fig. 10 Baicalein (BE) regulated ribosome-related pathways. (**A**-**F**) RT-qPCR were used to detect expression of *UTP21*, *NOG2*, *RCL1*, *IMP3*, *NOP1*, *RLP24* mRNA. All data are presented as mean ± SD: *$P < 0.05$, **$P < 0.01$, ***$P < 0.001$, ****$P < 0.0001$ vs. Control group

Discussion

Human fungal infections are rapidly increasing, with eukaryotic pathogens currently affecting billions globally and causing more than 1.5 million deaths annually (Brown et al. 2012). *Candida* spp. are the most significant fungal pathogens responsible for invasive infections (Brown et al. 2012). The CDC has identified *Candida* spp. as a serious threat to human health due to the significant rise in drug-resistant infections, especially those caused by non-albicans *Candida* species (Chowdhary et al. 2023).

Candida auris is a fungal pathogen that resists many conventional antifungal drugs, making it a significant threat to global human health. Since the first case was reported in Japan in 2009, *C. auris* infections have been documented in over 40 countries. The mortality rates for these infections range from 30% to 60% (Du et al. 2020). *C. auris* can cause outbreaks in healthcare facilities, particularly in nursing homes for the elderly, because it spreads efficiently through skin-to-skin contact (Ruiz-Gaitán et al. 2018; Chowdhary et al. 2023). *C. auris* is the first fungal pathogen known to exhibit significant and sometimes untreatable clinical drug resistance against all known antifungal classes, including azoles, AmB, and echinocandins (Chaabane et al. 2019; Chowdhary et al. 2023). It is crucial to explore new antifungal drugs to overcome the limited effectiveness, high levels of toxicity, and drug resistance linked with existing antifungal medications. In our previous studies, BE demonstrated potent antifungal activity against *C. auris*, and it was also observed that BE possesses the capability to induce cellular apoptosis and diminish yeast cell viability (Li et al. 2024). To better understand how BE works against *C. auris* by inducing apoptosis, we examined the characteristics related to yeast apoptosis.

Apoptosis is the earliest discovered type of regulated cell death, mediated by intracellular caspase-3 and caspase-7. These enzymes cleave different intracellular substrates. This process results in cell shrinkage, chromatin fragmentation, membrane blebbing, and the creation of membrane-wrapped vesicles (Ai et al. 2024).

Biofilm refers to a structured microbial community that emerges on abiotic or biological surfaces and is embedded within the extracellular matrix. It is an extracellular structure constituted by glycoproteins, carbohydrates, polysaccharides (Prasad et al. 2019). The biofilm formed by *C. auris* not only relies on the accumulation of yeast but also

consists of a certain amount of extracellular matrix (Larkin et al. 2017), and eventually forms a compact group structure, facilitating *C. auris* to survive for a prolonged period on the surface of the environment and evade the host. In SEM, both the control group and the groups treated with 7.4 μM and 14.8 μM BE, as well as 209 μm FLZ, *C. auris* exhibited a distinct oval-shaped yeast morphology. However, exposure to BE at concentrations of 29.6 μM and 59.2 μM led to notable changes in the topography of yeast cells, indicating that BE may trigger the apoptosis of *C. auris*.

PS is widely distributed in the medial part of eukaryotic cell membranes. PS evagination serves as an important characteristic of viable apoptosis, providing a crucial signal for apoptotic cells and phagocytes to identify and eliminate (Leventis et al. 2010). Based on the flow cytometry data, it was observed that *C. auris* cells exposed to 29.6μM and 59.2μM BE exhibited a significant presence of apoptotic cells (39.9% and 41.23% apoptotic), indicating that BE induced apoptosis in *C. auris* (Jia et al. 2019; Liu et al. 2022). Similarly, FLZ could also trigger early apoptosis in *C. auris*, albeit with less efficacy compared to BE.

Metacaspases constitute a distinct category of enzymes capable of regulating various cellular processes, including programmed cell death (PCD), like caspases (Tsiatsiani et al. 2011). Our findings demonstrated an increase in fluorescence quantity with the rise in BE concentration, indicating heightened metacaspase activity in cells treated with BE (14.8, 29.6, and 59.2 μM), but not in FLZ-treated cells (Jia et al. 2019; Liu et al. 2022).

ROS are generated through the incomplete reduction of molecular oxygen, encompassing superoxide anion (O_2-.), hydrogen peroxide (H_2O_2), hydroxyl radical (OH.), and singlet oxygen ($^1O_2$). ROS have the potential to induce various forms of cellular damage, particularly lipid peroxidation and membrane injury (Baud et al. 1986; Suski et al. 2012; Prasad et al. 2018). The ROS Assay Kit and SOSG were employed to evaluate the levels of extracellular ROS and $^1O_2$, as documented in the literature. Research has demonstrated that higher concentrations of BE increase the production of ROS and $^1O_2$ by *C. auris*, resulting in increased cellular damage. However, FLZ was not effective against *C. auris*.

Mitochondria are widely recognized as the primary source of ROS within the cell, contributing to various pathological conditions and aging. Prolonged elevation in ROS production rates leads to the accumulation of ROS-induced damage in DNA, proteins, and lipids, ultimately resulting in progressive cellular dysfunction (low mitochondrial membrane potential) and subsequent apoptosis, thereby increasing the overall likelihood of pathological conditions in an organism (Jia et al. 2019; Liu et al. 2022). The JC-1 enhanced mitochondrial membrane potential (MMP) assay kit can detect alterations in MMP. In our research, we observed a significant decrease in the MMP of *C. auris* when exposed to BE (29.6 and 59.2μM), indicating substantial damage to the mitochondria and initiation of early apoptosis in the cells. FLZ also induces a certain level of disruption in the MMP, albeit not as pronounced as BE.

Apoptosis includes cellular shrinkage, pyknosis (chromatin condensation), karyorrhexis (nuclear fragmentation), and subsequent DNA fragmentation (Majtnerová et al. 2018). Additionally, the DAPI staining solution effectively detects nuclear fragmentation, which was observed in our experiments. The results showed that with BE treatment at concentrations of 14.8, 29.6, and 59.2 μM, *C. auris* displayed noticeable nuclear contraction and fragmentation. In contrast, FLZ had minimal effect. DNA fragmentation occurs in the later stages of the apoptotic process (Majtnerová et al. 2018). The findings indicated that increasing concentrations of BE led to a greater production of DNA fragments in *C. auris* cells, while FLZ did not produce a similar effect.

Our transcriptome sequencing results indicate a significant impact on the ribosome and its related pathways after the BE intervention in *C. auris*. Ribosomes are essential cellular components composed of rRNA and ribosomal proteins (Liu et al. 2024). Numerous studies have established a close association between the ribosome and cell apoptosis. One study highlighted the importance of ribosomal UUA stalling caused by DNA damage as a trigger for apoptosis (Boon et al. 2024). And another research reveals that ribotoxic stress response (RSR) signaling via ZAK, rather than DNA damage response (DDR) signaling, is accountable for early apoptosis and cell-cycle arrest in response to ultraviolet (Sinha et al. 2024). Furthermore, we have previously noted that MMP and ROS are crucial indicators of apoptosis. A study demonstrated that ribosomal impairments lead to increased levels of mitochondrial reactive oxygen species (mROS), which activate cellular signaling pathways to manage ribosomal stress. Additionally, it was observed that reducing mROS levels or MMP exacerbated the growth of cells with defective ribosomes (Liu et al. 2024). Our study found that the differentially expressed genes were primarily enriched in ribosome biogenesis and ribosomes, as determined by KEGG functional annotation analysis. GO enrichment analysis indicated that BE may induce apoptosis in *C. auris* by affecting various processes, including ribosomal RNA processing, ncRNA processing, rRNA metabolism and nucleolus (Shan et al. 2023). Therefore, we selected six genes (*IMP3*, *NOP1*, *UTP21*, *NOG2*, *RLP24*, *RCL1*) with the most significant differences for RT-qPCR analysis, based on the heat map of differentially expressed genes. These ribosomal genes are critical to various biological processes, as supported by previous studies (Tollervey et al. 1991; Lee

et al., 1999; Billy et al. 2000; Saveanu et al. 2003; Honma et al. 2006; Zhang et al. 2014). RT-qPCR results indicated that all selected genes significantly decreased, aligning with the findings from our transcriptome sequencing study. Therefore, we infer that BE may impact ribosomal function and related pathways to facilitate apoptosis in *C. auris*.

Conclusions

Collectively, this study explored the mechanisms by which baicalein (BE) acts against *Candida auris*. Our findings indicate that BE may trigger apoptosis in *C. auris* by affecting ribosomal function and related pathways. This highlights the effectiveness of BE against this 'super fungus' and provides valuable insights for future prevention and treatment strategies aimed at *C. auris*.

Acknowledgements This work was supported by the National Natural Science Foundation of China (Grant Nos. 82374173, 81774034, 81573725), and the Key Research and Development Projects of Anhui Province (202104a07020020), the Key scientific research projects of Anhui Provincial Department of Education (KJ2021A0590).

Author contributions All the authors contributed extensively to the work presented in this manuscript. The study was conceived by LC and WCZ. Experimental procedures were carried out by LC, WH. Data analyses were performed by LC, WH, WJ, ZL, QW, WWF, WTM. The paper was written by LC, WCZ.

Funding This work was supported by the National Natural Science Foundation of China (Grant Nos. 82374173, 81774034，81573725), and the Key Research and Development Projects of Anhui Province (202104a07020020), the Key scientific research projects of Anhui Provincial Department of Education (KJ2021A0590).

Data availability No datasets were generated or analysed during the current study.

Declarations

Competing interests The authors declare no competing interests.

References

Ahmad S, Khan Z, Al-Sweih N, Alfouzan W, Joseph L (2020) *Candida Auris* in various hospitals across Kuwait and their susceptibility and molecular basis of resistance to antifungal drugs. Mycoses 63(1):104–112. https://doi.org/10.1111/myc.13022

Ai Y, Meng Y, Yan B, Zhou Q, Wang X (2024) The biochemical pathways of apoptotic, necroptotic, pyroptotic, and ferroptotic cell death. Mol Cell 84(1):170–179. https://doi.org/10.1016/j.molcel.2023.11.040

Baud L, Ardaillou R (1986) Reactive oxygen species: production and role in the kidney. Am J Physiol 251(5 Pt 2):F765–F776. https://doi.org/10.1152/ajprenal.1986.251.5.F765

Billy E, Wegierski T, Nasr F, Filipowicz W (2000) Rcl1p, the yeast protein similar to the RNA 3'-phosphate cyclase, associates with U3 snoRNP and is required for 18S rRNA biogenesis. EMBO J 19(9):2115–2126. https://doi.org/10.1093/emboj/19.9.2115

Bing J, Guan Z, Zheng T, Ennis CL, Nobile CJ, Chen C, Chu H, Huang G (2024) Rapid evolution of an adaptive multicellular morphology of *Candida Auris* during systemic infection. Nat Commun 15(1):2381. https://doi.org/10.1038/s41467-024-46786-8

Boon NJ, Oliveira RA, Körner PR, Kochavi A, Mertens S, Malka Y, Voogd R, van der Horst SEM, Huismans MA, Smabers LP, Draper JM, Wessels LFA, Haahr P, Roodhart JML, Schumacher TNM, Snippert HJ, Agami R, Brummelkamp TR (2024) DNA damage induces p53-independent apoptosis through ribosome stalling. Science 384(6697):785–792. https://doi.org/10.1126/science.adh7950

Brown GD, Denning DW, Gow NA, Levitz SM, Netea MG, White TC (2012) Hidden killers: human fungal infections. Sci Transl Med 4(165):165rv13. https://doi.org/10.1126/scitranslmed.3004404

Chaabane F, Graf A, Jequier L, Coste AT (2019) Review on Antifungal Resistance mechanisms in the Emerging Pathogen *Candida Auris*. Front Microbiol 10:2788. https://doi.org/10.3389/fmicb.2019.02788

Chowdhary A, Jain K, Chauhan N (2023) *Candida Auris* Genetics and Emergence. Annu Rev Microbiol 77:583–602. https://doi.org/10.1146/annurev-micro-032521-015858

Dai BD, Cao YY, Huang S, Xu YG, Gao PH, Wang Y, Jiang YY (2009) Baicalein induces programmed cell death in *Candida albicans*. J Microbiol Biotechnol 19(8):803–809

Du H, Bing J, Hu T, Ennis CL, Nobile CJ, Huang G (2020) *Candida Auris*: Epidemiology, biology, antifungal resistance, and virulence. PLoS Pathog 16(10):e1008921. https://doi.org/10.1371/journal.ppat.1008921

Fu Z, Lu H, Zhu Z, Yan L, Jiang Y, Cao Y (2011) Combination of baicalein and amphotericin B accelerates *Candida albicans* apoptosis. Biol Pharm Bull 34(2):214–218. https://doi.org/10.1248/bpb.34.214

Honma Y, Kitamura A, Shioda R, Maruyama H, Ozaki K, Oda Y, Mini T, Jenö P, Maki Y, Yonezawa K, Hurt E, Ueno M, Uritani M, Hall MN, Ushimaru T (2006) TOR regulates late steps of ribosome maturation in the nucleoplasm via Nog1 in response to nutrients. EMBO J 25(16):3832–3842. https://doi.org/10.1038/sj.emboj.7601262

Jia C, Zhang J, Yu L, Wang C, Yang Y, Rong X, Xu K, Chu M (2019) Antifungal Activity of Coumarin against *Candida albicans* is related to apoptosis. Front Cell Infect Microbiol 8:445. https://doi.org/10.3389/fcimb.2018.00445

Kaczanowski S (2016) Apoptosis: its origin, history, maintenance and the medical implications for cancer and aging. Phys Biol 13(3):031001. https://doi.org/10.1088/1478-3975/13/3/031001

Larkin E, Hager C, Chandra J, Mukherjee PK, Retuerto M, Salem I, Long L, Isham N, Kovanda L, Borroto-Esoda K, Wring S, Angulo D, Ghannoum M (2017) The Emerging Pathogen Candida Auris: growth phenotype, virulence factors, activity of antifungals, and Effect of SCY-078, a Novel Glucan synthesis inhibitor, on growth morphology and biofilm formation. Antimicrob Agents Chemother 61(5):e02396–e02316. https://doi.org/10.1128/AAC.02396-16

Lee SJ, Baserga SJ (1999) Imp3p and Imp4p, two specific components of the U3 small nucleolar ribonucleoprotein that are essential for pre-18S rRNA processing. Mol Cell Biol 19(8):5441–5452. https://doi.org/10.1128/MCB.19.8.5441

Lei J, Huang J, Xin C, Liu F, Zhang J, Xie Y, Mao Y, Chen W, Song Z (2023) Riboflavin targets the Cellular Metabolic and Ribosomal pathways of *Candida albicans* in Vitro and exhibits Efficacy against Oropharyngeal Candidiasis. Microbiol Spectr 11(1):e0380122. https://doi.org/10.1128/spectrum.03801-22

Leventis PA, Grinstein S (2010) The distribution and function of phosphatidylserine in cellular membranes. Annu

Rev Biophys 39:407–427. https://doi.org/10.1146/annurev.biophys.093008.131234

Li C, Wang J, Li H, Wang Y, Wu H, Wei W, Wu D, Shao J, Wang T, Wang C (2024) Suppressing the virulence factors of *Candida Auris* with baicalein through multifaceted mechanisms. Arch Microbiol 206(8):349. https://doi.org/10.1007/s00203-024-04038-9

Liu X, Guo C, Zhuang K, Chen W, Zhang M, Dai Y, Tan L, Ran Y (2022) A recyclable and light-triggered nanofibrous membrane against the emerging fungal pathogen *Candida Auris*. PLoS Pathog 18(5):e1010534. https://doi.org/10.1371/journal.ppat.1010534

Liu L, Wu Y, Liu K, Zhu M, Guang S, Wang F, Liu X, Yao X, He J, Fu C (2024) The absence of the ribosomal protein Rpl2702 elicits the MAPK-mTOR signaling to modulate mitochondrial morphology and functions. Redox Biol 73:103174. https://doi.org/10.1016/j.redox.2024.103174

Majtnerová P, Roušar T (2018) An overview of apoptosis assays detecting DNA fragmentation. Mol Biol Rep 45(5):1469–1478. https://doi.org/10.1007/s11033-018-4258-9

Prasad A, Sedlářová M, Pospíšil P (2018) Singlet oxygen imaging using fluorescent probe Singlet Oxygen Sensor Green in photosynthetic organisms. Sci Rep 8(1):13685. https://doi.org/10.1038/s41598-018-31638-5

Prasad R, Nair R, Banerjee A (2019) Emerging mechanisms of Drug Resistance in *Candida albicans*. Prog Mol Subcell Biol 58:135–153. https://doi.org/10.1007/978-3-030-13035-0_6

Qi Y, Li X, Chang C, Xu F, He Q, Zhao Y, Wu L (2017) Ribosomal protein L23 negatively regulates cellular apoptosis via the RPL23/Miz-1/c-Myc circuit in higher-risk myelodysplastic syndrome. Sci Rep 7(1):2323. https://doi.org/10.1038/s41598-017-02403-x

Ruiz-Gaitán A, Moret AM, Tasias-Pitarch M, Aleixandre-López AI, Martínez-Morel H, Calabuig E, Salavert-Lletí M, Ramírez P, López-Hontangas JL, Hagen F, Meis JF, Mollar-Maseres J, Pemán J (2018) An outbreak due to *Candida Auris* with prolonged colonisation and candidaemia in a tertiary care European hospital. Mycoses 61(7):498–505. https://doi.org/10.1111/myc.12781

Satoh K, Makimura K, Hasumi Y, Nishiyama Y, Uchida K, Yamaguchi H (2009) *Candida Auris* sp. nov., a novel ascomycetous yeast isolated from the external ear canal of an inpatient in a Japanese hospital. Microbiol Immunol 53(1):41–44. https://doi.org/10.1111/j.1348-0421.2008.00083.x

Saveanu C, Namane A, Gleizes PE, Lebreton A, Rousselle JC, Noaillac-Depeyre J, Gas N, Jacquier A, Fromont-Racine M (2003) Sequential protein association with nascent 60S ribosomal particles. Mol Cell Biol 23(13):4449–4460. https://doi.org/10.1128/MCB.23.13.4449-4460.2003

Shan L, Xu G, Yao RW, Luan PF, Huang Y, Zhang PH, Pan YH, Zhang L, Gao X, Li Y, Cao SM, Gao SX, Yang ZH, Li S, Yang LZ, Wang Y, Wong CCL, Yu L, Li J, Yang L, Chen LL (2023) Nucleolar URB1 ensures 3' ETS rRNA removal to prevent exosome surveillance. Nature 615(7952):526–534. https://doi.org/10.1038/s41586-023-05767-5

Sinha NK, McKenney C, Yeow ZY, Li JJ, Nam KH, Yaron-Barir TM, Johnson JL, Huntsman EM, Cantley LC, Ordureau A, Regot S, Green R (2024) The ribotoxic stress response drives UV-mediated cell death. Cell, S0092-8674(24)00527-0. Advance online publication https://doi.org/10.1016/j.cell.2024.05.018

Suski JM, Lebiedzinska M, Bonora M, Pinton P, Duszynski J, Wieckowski MR (2012) Relation between mitochondrial membrane potential and ROS formation. Methods Mol Biol (Clifton N J) 810:183–205. https://doi.org/10.1007/978-1-61779-382-0_12

Tian H, Qu S, Wang Y, Lu Z, Zhang M, Gan Y, Zhang P, Tian J (2017) Calcium and oxidative stress mediate perillaldehyde-induced apoptosis in *Candida albicans*. Appl Microbiol Biotechnol 101(8):3335–3345. https://doi.org/10.1007/s00253-017-8146-3

Tollervey D, Lehtonen H, Carmo-Fonseca M, Hurt EC (1991) The small nucleolar RNP protein NOP1 (fibrillarin) is required for pre-rRNA processing in yeast. EMBO J 10(3):573–583. https://doi.org/10.1002/j.1460-2075.1991.tb07984.x

Tsiatsiani L, Van Breusegem F, Gallois P, Zavialov A, Lam E, Bozhkov PV (2011) Metacaspases Cell Death Differ 18(8):1279–1288. https://doi.org/10.1038/cdd.2011.66

Wu Y, Chen Y, Lu H, Ying C (2023) Miltefosine exhibits fungicidal activity through oxidative stress generation and Aif1 activation in *Candida albicans*. Int J Antimicrob Agents 62(1):106819. https://doi.org/10.1016/j.ijantimicag.2023.106819

Wu H, Li C, Wang Y, Zhang M, Wu D, Shao J, Wang T, Wang C (2024) Transcriptomics reveals Effect of Pulsatilla Decoction Butanol Extract in alleviating Vulvovaginal Candidiasis by inhibiting Neutrophil Chemotaxis and Activation via TLR4 Signaling. Pharmaceuticals (Basel Switzerland) 17(5):594. https://doi.org/10.3390/ph17050594

Yi YW, You KS, Park JS, Lee SG, Seong YS (2021) Ribosomal protein S6: a potential therapeutic target against Cancer? Int J Mol Sci 23(1):48. https://doi.org/10.3390/ijms23010048

Zhang C, Lin J, Liu W, Chen X, Chen R, Ye K (2014) Structure of Utp21 tandem WD domain provides insight into the organization of the UTPB complex involved in ribosome synthesis. PLoS ONE 9(1):e86540. https://doi.org/10.1371/journal.pone.0086540